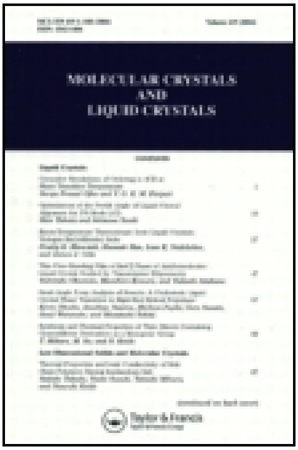

Molecular Crystals and Liquid Crystals

Publication details, including instructions for authors and subscription information:
http://www.tandfonline.com/loi/gmcl20

Polarized Near-Field Optical Study of Cavity Modes of Lasing and Amplified Spontaneous Emissions

Akihiro Tomioka [a] , Tooru Motokubota [b] , Yasuaki Itakura [b] & Sinji Kinosita [b]

[a] Osaka Electro-Communication University and Academic Frontier Promotion Center, Osaka, Japan

[b] Osaka Electro-Communication University, Osaka, Japan

Version of record first published: 12 Mar 2007

To cite this article: Akihiro Tomioka, Tooru Motokubota, Yasuaki Itakura & Sinji Kinosita (2007): Polarized Near-Field Optical Study of Cavity Modes of Lasing and Amplified Spontaneous Emissions, Molecular Crystals and Liquid Crystals, 463:1, 73/[355]-81/[363]

To link to this article: http://dx.doi.org/10.1080/15421400601021539

Mol. Cryst. Liq. Cryst., Vol. 463, pp. 73/[355]–81/[363], 2007

ISSN: 1542-1406 print/1563-5287 online
DOI: 10.1080/15421400601021539

Polarized Near-Field Optical Study of Cavity Modes of Lasing and Amplified Spontaneous Emissions

Akihiro Tomioka
Osaka Electro-Communication University and Academic Frontier Promotion Center, Osaka, Japan

Tooru Motokubota
Yasuaki Itakura
Sinji Kinosita
Osaka Electro-Communication University, Osaka, Japan

To elucidate the optical coupling nature of near-field scanning optical microscope (NSOM) probes we observed by a NSOM the lasing field of commercial laser diodes (LDs) on their cleaved surface that was expected to be an ideal single TE_{00} mode and be polarized perpendicular to the probe axis. A clear dark region was observed at the lasing active region of the LD, indicating that the optical probe coupled only the target near-field polarized parallel to the probe's long axis. Many concentric bright rings, detected in the near-field emission profile extending outside of the optical guide layer, should be polarized perpendicular to the TE_{00} mode, and were ascribed to amplified spontaneous emissions from recombination between an electron and a light hole, based on the symmetry of radiation field. Another possibility was an optical coupling between the optical probe and the laser diode cavity, which might modify the original field distribution inside the laser diode cavity. In both cases the observation suggests that a near-field probe works as a novel tool to manipulate the cavity electromagnetic field, which is a common issue to many applications of cavities made from organic ultrathin films.

Keywords: cavity mode; laser diode; near field; non radiating; NSOM; quantum well

This work was supported partly by the Academic Frontier Promotion Project of the Ministry of Education, Culture, Sports, Science and Technology and partly by the Science Research Promotion Fund of Japan Private School Promotion Foundation. We express our gratitude to Professor Wataru Susaki for the discussions on possible mode field inside the quantum wells and to Professor Hiroyuki Enomoto for assistance on the proper temperature control of the LD chip.

Address correspondence to Akihiro Tomioka, Osaka Electro-Communication University, 18-8 Hatucho, Neyagawa, Osaka 572-8530, Japan. E-mail: tomioka@isc.osakac.ac.jp

INTRODUCTION

Many waveguides [1] are reported to be fabricated from organic ultra-thin films and the manipulation of the existence of useful modes is major concern. However the optical coupling to these nanostructures is still a tough problem although it is the important interface between the novel nanostructures and the ordinary-scale macrostructures fabricated easily with conventional techniques. In the present paper we study the characteristics of the near-field probe of near-field scanning optical microscope (NSOM), especially concerning on what optical modes of the target nanostructures these probes can couple with. The majority of the research using near-field probes is a microscopy and concerns only about the high-resolution they bring about. We believe that it has much importance whether they can detect all the optical modes within the target and what difference the non-radiating near-fields have from the conventional propagating light.

As a target to study this, we adopt conventional laser diode (LD) chips whose nanostructures are well-defined and whose optical characteristics of the cavity modes are fully studied. An NSOM study is conducted to obtain the near-field emission profile from the cleaved LD surface [2–9] and to obtain the mapping of photocurrent induced by an optical near-field of the probe [10], leading to the first report on the coupling and non-coupling of the probe and the LD cavity modes.

MATERIALS AND METHODS

In the present research we used commercially available AlGaInP index-guided laser diodes with double hetero quantum well (QW) structures, $P_0 = 5\,\mathrm{mW}$ Sanyo DL3149-054, $P_0 = 7\,\mathrm{mW}$ Sanyo DL3149-057, $P_0 = 60\,\mathrm{mW}$ Mitsubishi ML60124R, as target specimen. To place the NSOM probe tip in the vicinity of the target cleaved surface of the LD semiconductor chip, we needed to open the LD's sealed can and make the cleaved surface exposed to the ambient atmosphere. We needed some strategies how to place the probe tip within the Piezo scanner's movable range (36 μm by 36 μm) manually without colliding the optical probe tip with e.g. large silicon substrate standing vertically or thin gold wires winding around the chip [11]. The LD was attached to a copper specimen block fabricated specifically with enough heat capacitance to absorb the heat from the LD in operation. We needed to modulate the LD emission via its driving current and detect the lasing field with a lock-in amplifier. An optical spectrum of local fields picked up by the probe was obtained by a blazed grating polychromater equipped with a high efficiency back-illuminated cooled

CCD camera with on-chip multiplication capability of the stored and accumulated electrons.

To map the photocurrent induced by an optical near-field the LD chip surface was locally photoexcited by the near-field of the probe tip and the resulting photocurrent was detected by a lockin amplifier.

RESULTS AND DISCUSSION

Figure 1(b) shows the driving current vs. the optical output curve of a 5 mW Sanyo LD. The optical output increases abruptly at 29 mA, which is consistent with the manufacturer's specification of typical threshold current of 30 mA. Figure 1(a) shows the height image of the cleaved surface of the LD chip with the anode silicon substrate (black region) at the right hand side. The cathode metal layer is located at 60 μm apart from the right edge, out of view in the left. When 30 mA (just above the lasing threshold), and then 35 mA, of the driving current was injected through the electrodes, a single broad emission profile was observed by the NSOM, in Figures 1(e) and 1(f), respectively, elongated in the direction parallel to the quantum wells (QWs). The full width at the intensity half maximum (FWHM) was 3 μm and 2.5 μm, respectively, which reflects the longitudinal multimode mixture and the pure single-mode operation, respectively. Their mode difference was confirmed by a high-resolution optical spectrum analyzer (data not shown). The intensity peak was located at 4 μm from the chip right edge, which was consistent with the far-field observation by a high-magnification microscope. The distribution in the direction perpendicular to the QW was wider in the right half, which may be ascribed to an asymmetric charge distribution across the QW. The difference in refractive index is expected to be much smaller than 10% and therefore can not explain the asymmetric spread of the optical field. The FWHM parallel to the QW was about 5 μm, which may reflect the driving current confinement due to the electrode ridge structure. Since the heat conduction was insufficient between the LD base plate and the copper heat sink, the probe position control was unstable in this experiment, leading to some artificial stripes in Figures 1(e) and 1(f) running in the first scanning direction (horizontal). In order to avoid the probe collision to the LD chip the spatial separation was kept at 1 μm. The images of Figures 1(e) and 1(f) should therefore be interpreted as the medium between the near-field and the far-field.

Next, to compare the emission profile with those of high-power LDs [Mitsubishi 60 mW LD, Figure 2(a)], the contact with the copper heat sink was improved and the heat sink temperature was monitored. The temperature raise was only few degrees after 1 hour operation at

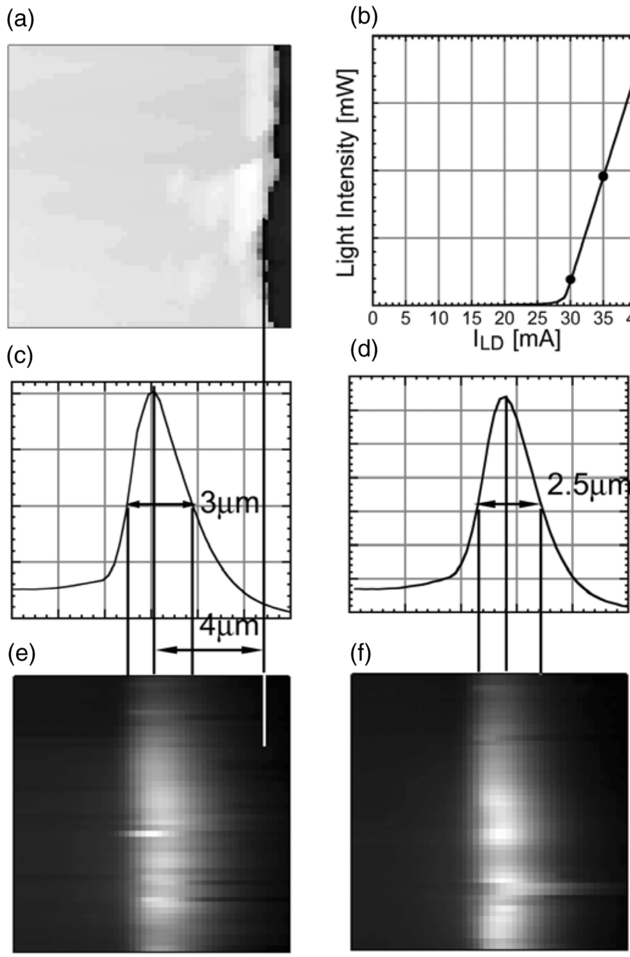

FIGURE 1 NSOM images of a 5 mW Sanyo LD observed at the probe-LD chip separation of 1 µm. The LD was driven by 30 mA, just above the lasing threshold, and 35 mA, at a single-mode lasing level, as marked by two circles in the current vs. light output curve of (b). (e) and (f) The NSOM images of the detected optical field at the driving current of 30 mA and 35 mA, respectively. The vertical white line shown in (e) indicates the LD chip right edge deduced from the simultaneously obtained topography of (a). (c) and (d) The intensity line profile of the images (e) and (f), respectively, along the horizontal line across the center. FWHM was indicated by an arrow across the peak position.

33 mA of the driving current, which was a typical experimental condition to scan a large area. A stable control of probe position enabled the scanning at the probe separation of 100 nm, which should produce

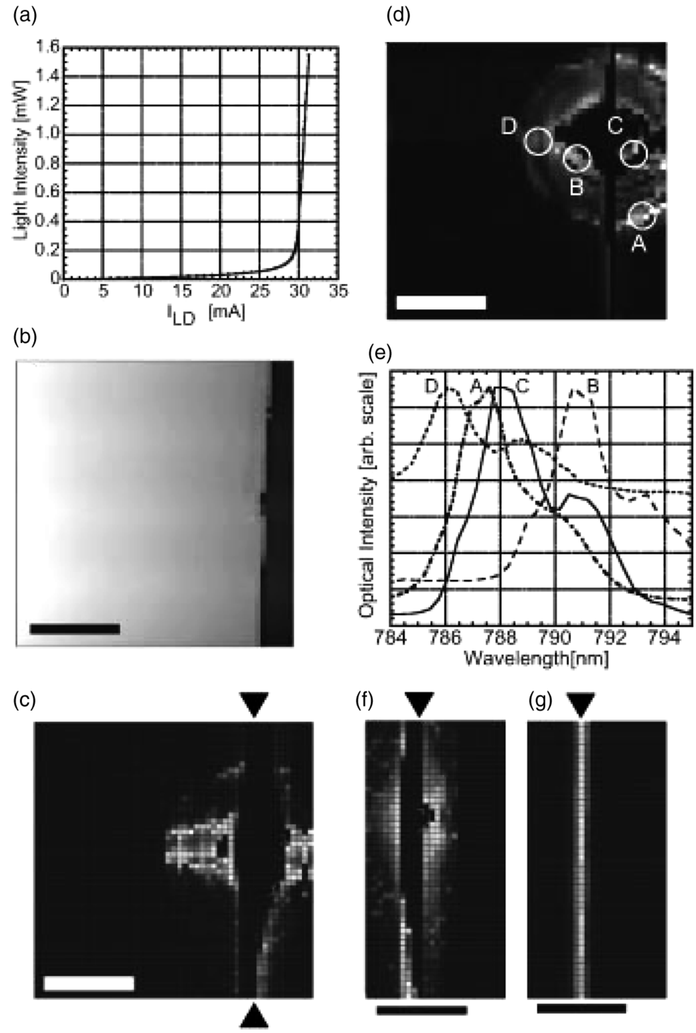

FIGURE 2 NSOM images of a 60 mW Mitsubishi LD observed at the probe-LD chip separation of 100 nm. (a) The driving current vs. light output curve, (b) topography of the LD surface, (c), (d) and (f) the optical near-field image observed at the driving current of 25 mA, 33 mA and 30 mA, respectively. (e) The optical spectra of the local field detected at the spots marked as A, B, C and D in (d). (g) The mapping of electric current produced by the free carriers excited by an optical near-field. No bias voltage was applied. Only part of the map was shown in (f) and (g). All the scale bars indicate 10 μm. The deduced location of the LD active region is indicated by a triangle in (c), (f) and (g).

a true near-field image. The resulting emission profile [Figs. 2(c) and 2(d)] showed no intensity in the LD active region. The Si avalanche photodiode used for detection had sufficient sensitivity over the whole visible wavelength. Optical field was detected only outside of the guide layer extending out over 5 μm or more. Below the threshold current it appeared as a continuous profile while above the threshold it appeared as concentric rings with multiple spots along them. After the scanning, the probe was repositioned at these spots and the spectrum of the detected optical field was recorded by a spectrometer with wavelength resolution of 0.4 nm [Fig. 2(e)]. The strong spots, as indicated as A, B and C in Figure 2(d), showed narrow peaks with full width about 3 nm, which implies that these mode fields correspond to amplified spontaneous emissions (ASEs). At the same driving current of 33 mA, the far-field observation by a high-resolution optical spectrum analyzer showed a 780 nm single-mode lasing and only a faint power at several other neighboring longitudinal modes with multiples of 0.1 nm apart; there were no noticeable modes above 786 nm. This observation suggests that the ASEs described above may be non-radiating modes that only a near-field probe can detect. Furthermore, there is a possibility that a near-field probe might modify the LD cavity inducing these ASE modes and that these ASE modes did not exist without the probe in a vicinity of the chip surface.

To elucidate the nature of the dark region along the LD active region, the LD chip surface was photoexcited by a probe's near-field and the resulting photocurrent was recorded as a function of the probe location. The obtained photocurrent mapping [Fig. 2(g)] clearly showed the location of the active region. The spatial spread of 0.6 μm perpendicular to the QW represented the diffusion length of the photoproduced free carriers. The diffusion length was far shorter than those shown in Figure 1 because no potential gradient was imposed in the photocurrent experiment.

The white stripe representing the intense photocurrent in Figure 2(g) corresponds well to the dark stripe in the optical emission profile [Fig. 2(f)]. Since the experiments of Figure 2(f), and then 2(g), were performed consecutively, the dark stripe in Figure 2(f) did not mean the deterioration of the active region. The far-field image still showed a single strong lasing that should exist in the experiments of Figures 2(c) through 2(f). The dark stripe, therefore, should be interpreted as non-coupling of the probe with this radiating laser mode. This lasing single-mode is known to be the TE_{00} mode [12] whose electric field is ideally polarized parallel to the QW layer [in the vertical direction in Figure 2(f)] and also parallel to the LD chip surface. The near-field profiles remained identical even when the target LD chip was rotated by 90°, which means that the optical probe can not couple to the radiating field with the electric vector polarized perpendicular to the probe axis. This model of the probe-field coupling is consistent with the previous observation [13] that the fluorescence of the organic dye aggregates was not detected by an NSOM probe when the transition moment of the dyes were aligned perpendicular to the probe axis.

To make sure that the observation that the probe couples only to the longitudinal electric field was not due to the properties of a specific LD, a medium-power 7 mW Sanyo LD was then scanned by the NSOM

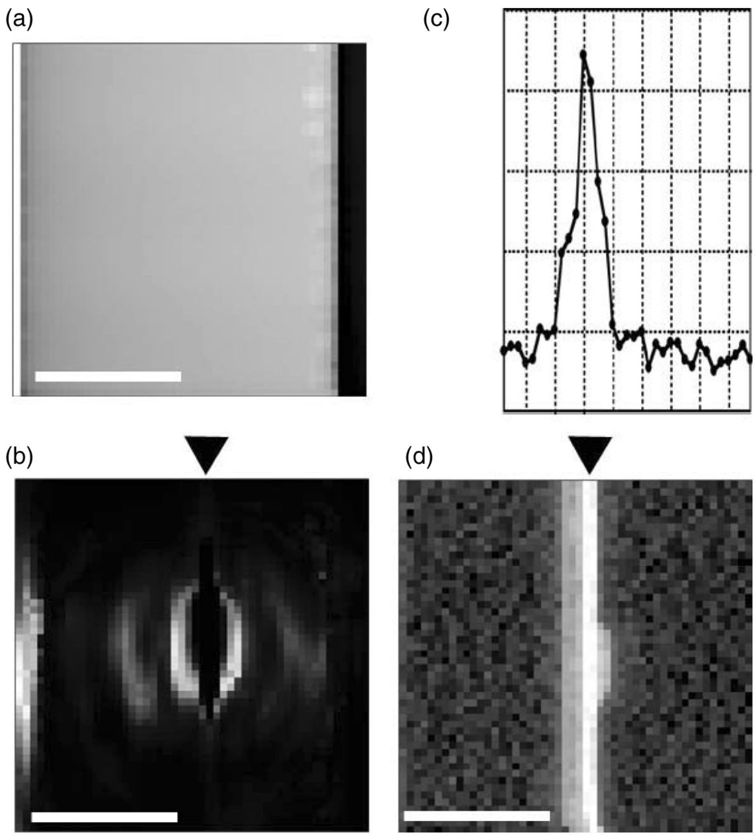

FIGURE 3 NSOM images of a 7 mW Sanyo LD observed at the probe-LD chip separation of 100 nm. (a) The topography of the LD surface, (b) the optical near-field image observed at the driving current of 30 mA, (d) the mapping of optical near-field excited current. The deduced location of the LD active region is indicated by a triangle in (b) and (d). (c) The horizontal line profile across the center of (d). The scale bars indicate 10 μm.

at the same probe-surface separation of 100 nm. A dark stripe was consistently observed in the emission profile [Fig. 3(b)] and the location of this stripe was confirmed to correspond to the LD active region by a NSOM mapping of the near-field (photo)excited current [Fig. 3(d)]. The line profile [Fig. 3 (c)] across the center in the direction perpendicular to the QW indicates the wider full width of 1.5 μm where the electrode ridge structure does not affect the current distribution.

The many spots along concentric rings detected in the near-field emission profiles may be originated from recombination between an electron and a light hole rather than an electron and a heavy hole. Established discussions [12,14] concerning the symmetry of these different types of radiative recombination inside semiconductor QWs argue that electron/light hole recombination should produce photons polarized perpendicular to the electron $\boldsymbol{k}$-vector that points perpendicular to the quantum well layer. This prediction supports our interpretation of concentric modes being observed only by the NSOM that has the coupling capability only with the optical electric field parallel to the probe axis.

CONCLUSIONS

Spatial emission profile of LDs was observed by an NSOM and it showed a single broad peak, which was in good agreement with the far-field observation, when the probe was separated by 1 μm from the LD chip surface. This single peak did not observed, however, when the probe separation was 100 nm, i.e. in the near-field regime, and many spots appeared instead along concentric rings outside of the active region showing sharp spectra like ASEs at far longer wavelength than the familiar sub-lasing multimodes. The inability to couple with the TE_{00} mode might be ascribed to the characteristics of the near-field probe, which is consistent with our previous report. The possible ASE modes observed only by the near-field probe opens up new measures to detect non-radiating hidden modes inside cavities. Furthermore it suggests that the probe may work as a tool to modify and create optical fields inside the cavity.

REFERENCES

[1] McGehee, M. D. & Heeger, A. J. (2000). *Adv. Mater.*, *12*, 1655.

[2] Saito, N., Sato, F., Takizawa, K., Kusano, J., Okumura, H., Aida, T., Saiki, T., & Ohtsu, M. (1997). *Jpn. J. Appl. Phys.*, *36*, L896.

[3] Rhodes, G. H. V., Pomeroy, J. M., Unlu, M. S., Goldberg, B. B., Knopp, K. J., & Christensen, D. H. (1998). *Appl. Phys. Lett.*, *72*, 1811.

[4] Knopp, K. J., Christensen, D. H., Rhodes, G. H. V., Pomeroy, J. M., Goldberg, B. B., & Unlu, M. S. (1999). *J. Lightwave Tech*., *17*, 1429.
[5] Buratto, S. K., Hsu, J. W. P., Trautman, J. K., Betzig, E., Bylsma, R. B., Bahr, C. C., & Cardillo, M. J. (1994). *J. Appl. Phys*., *76*, 7720.
[6] Vertikov, A., Nurmikko, A. V., Doverspike, K., Bulman, G., & Edmond, J. (1998). *Appl. Phys. Lett*., *73*, 493.
[7] Young, D. K., Mack, M. P., Abare, A. C., Hansen, M., Coldren, L. A., Denbaas, S. P., Hu, E. L., & Awschalom, D. D. (1999). *Appl. Phys. Lett*., *74*, 2349.
[8] Vertikov, A., Ozden, I., & Nurmikko, A. V. (1999). *Appl. Phys. Lett*., *74*, 850.
[9] Kaneta, A., Okamoto, K., Kawakami, Y., Fujita, S., Marutsuki, G., Narukawa, Y., & Mukai, T. (2002). *Appl. Phys. Lett*., *81*, 4353.
[10] Buratto, S. K., Hsu, J. W. P., Betzig, E., Trautman, J. K., Bylsma, R. B., Bahr, C. C., & Cardillo, M. J. (1994). *Appl. Phys. Lett*., *65*, 2654.
[11] Motokubota, T., Tomioka, A., Itakura, Y., Kawabata, M., & Kinosita, S. (2005). *Int. Congr. Thin Films Int. Conf. Atom. Controlled Surf., Interfaces and Nanostruct*., Stockholm.
[12] Zory, P. S. Jr., ed., (1993). *Quantum Well Lasers*, Academic Press: San Diego, USA, Although the Figures 9 and 10 in Chap 1 treat the light incidence case, the dependence of the transition strength on angle between the electron's $\boldsymbol{k}$ vector and the light polarization is the same as the case of light emission.
[13] Tomioka, A., Ido, Y., Itakura, Y., & Motokubota, T. (2006). *Jpn. J. Appl. Phys*., *45*, 417.
[14] Jones, G. & O'Reilly, E. P. (1993). *IEEE J. Quant. Electr*., *29*, 1344–1354.